

Electronic Supplementary Information

Interlayer modified two-dimensional layered hexaniobate $K_4Nb_6O_{17}$ as anode materials for lithium-ion batteries

Satheeshkumar Elumalai^{*a}, Selvamani Vadivel^b and Masahiro Yoshimura^{*a, c}

^a*Department of Material Science and Engineering, National Cheng Kung University, Tainan 701, Taiwan. E-mail: analyticalsathi@gmail.com (S.E.); yoshimura@mssl.titech.ac.jp (M.Y.)*

^b*CSIR-CECRI, Karaikudi 630 006, Tamil Nadu, India.*

^c*Professor Emeritus, Materials and Structures Laboratory, Tokyo Institute of Technology, Tokyo 152-8550, Japan.*

†These authors (S.E. and S.V.) are equally contributed to this research.

‡The author (S.V.) present address: Department of Chemical and Biomolecular Engineering, Vidyasirimedhi Institute of Science and Technology (VISTEC), Rayong, 21210, Thailand.

Experimental methods

Material. Potassium carbonate (K_2CO_3) and Niobium (V) oxide (Nb_2O_5) was purchased from Sigma-Aldrich. The pristine layered hexaniobate ($K_4Nb_6O_{17}$) powder was used for the interaction of amino acids in water, such as Glycine (Gly). The hydrochloric acids (HCl) were received from TCI (Japan). All these chemicals were used as received without further treatment.

Solid-state synthesis of layered hexaniobate $K_4Nb_6O_{17}$ (LH). The 3:2 mmol ratio of K_2CO_3 (3.157 g) and Nb_2O_5 (8.127 g) were used as starting materials for the solid-state synthesis of pristine layered hexaniobate $K_4Nb_6O_{17}$ (LH). Both are mixed and ground in mortar for 30 min, during mixing a small volume (10 μ L, 5-time repeats) of n-hexane solvent, then calcinated at 1200° C for 48 h using Pt crucible.

Preparation of protonated LH (or PLH sample). About 2.0 g of pristine LH powder was added in 40 mL of 2 M HCl solution and stirred at 600 rpm for 3 days to exchange K^+ ions by H^+ ions (as H_3O^+) in interlayer-I, as resulting interlayer-I became a hydrate one (hydrophilic), whereas interlayer-II always remains as anhydrous one (hydrophobic, **Figure S1**). The H^+ ions exchanged pristine layered hexaniobate $K_4Nb_6O_{17}$ (LH) sample (hereafter called as protonated LH or PLH sample) were obtained by centrifugation at 4,000 rpm for 30 min and washing several times with distilled water until to reaches the pH 7 (pH of the supernatant was monitored for each wash) and dried at 40° C in vacuum.

Glycine intercalated $K_4Nb_6O_{17}$. About 1.0 wt% of amino acids, glycine (abbreviated as Gly) solution were prepared in 40 mL of distilled water. Before the intercalation of Gly into pristine layered hexaniobate $K_4Nb_6O_{17}$ (LH), the aqueous amino acids solution (pH of 1.0 wt% Gly in water is 6.40) was further sonicated in a bath sonicator (Bandelin-Sonorex Digitec, DT 514, 215 W, frequency 60 Hz, Germany) for 10 min for the complete dissolution. 0.250 g powder of both LH and PLH samples were independently added into the 1 wt% aqueous glycine solution and stirring at 500 rpm for 24 h at room temperature in a dark room. The resulting glycine-intercalated samples were obtained by centrifugation at 6,000 rpm for 60 min and washing with distilled water several times to remove an unreacted Gly and dried at 40 °C in the vacuum.

Characterization. A powder of pristine LH, protonated LH (PLH) and Gly intercalated PLH (Gly@PLH) samples were deposited onto the Si substrate and dried at 40 °C for 24 h prior to record the diffraction pattern using the X-ray diffractometer (Bruker new D8 ADVANCE instrument equipped with a monochromatic Cu $K\alpha$ radiation with a wavelength of 0.15418 nm, which is operated at 40 kV and 40 mA) measurement. The diffuse reflectance UV-visible (DR-UV-Vis spectroscopy) spectra of pristine LH, protonated LH (PLH) and Gly@PLH samples (PerkinElmer LAMDA 1050) were recorded by absorbance spectrometer with 1 cm optical path length cell. Fourier-transformed infrared (FT-IR) spectroscopy with Diamond-KRS-5 ATR mode (PerkinElmer Frontier-

FTIR, UK) was used for recording spectra in a range of 400 to 4,000 cm^{-1} with averaging 64 scans at 4 cm^{-1} resolution. The Raman spectra were measured on a RamanScope SENTERRA II (Bruker) with 532 nm excitation wavelength laser. For Raman measurements, the samples were deposited onto the glass substrate and recorded using a thermoelectric-cooled CCD array detector (Andor, DU420A-OE-152). The Raman signal was transferred through a 50 μm slit of a spectrometer and the spectral resolution of the spectrograph at 4 cm^{-1} across the Raman data acquired. The spectral acquisition time was 5s for all the samples with 2 accumulations averaged. The scanning electron micrograph images were obtained by a field emission scanning electron microscopy (FE-SEM, JEOL, JSM-7610F). Transmission electron microscopy (TEM, JEOL JEM-ARM200F, Japan) was used to study morphology before and after the intercalation of Gly into $\text{K}_4\text{Nb}_6\text{O}_{17}$. For the TEM sample preparation, all the samples were prepared by drop-casting onto a carbon film-coated 300 square mesh copper grid and dried at room temperature overnight in N_2 atmosphere. The high-resolution X-ray photoelectron spectroscopy (XPS) measurements were carried out on a JEOL XPS spectrometer (JPS-9019MC, Japan) for the powdered samples mounted on carbon tape using a monochromatic Mg $\text{K}\alpha$ source (25 W, $h\nu = 1253.6$ eV) and an energy resolution of 1 eV. All the XPS spectra were charge correction aligned on the binding energy scale referenced to the C 1s peak at 284.8 eV, and a PF4 software was used for the deconvolution of the narrow-scan XPS spectra.

Electrochemical characterization. The reversible lithium intercalation properties of the newly synthesized materials were studied by employing standard CR-2032 coin-type cell coupled with metallic lithium. The electrodes were prepared by a typical slurry based casting method. The active substance was hand-milled with a conductive super P and PVDF binder in the weight ratio of 70:20:10, followed by dispersing in the N-methyl pyrrolidone (NMP) solvent. The obtained uniform slurry was cast over the degreased copper foil (9 μm) and dried at 120 $^\circ\text{C}$ under vacuum. The calendered electrode was cut into 2 cm^2 disk, and the active material loading was in the range of 2.3 to 2.5 mg. The coin cell was fabricated by stacking the working electrode with polypropylene

separator (Celgard) wetted in the conventional electrolyte (1.0 M LiPF₆ in EC: DEC, Solvionic) and the surface polished lithium metal, in an Argon filled glove box (MBRAUN UNILAB), where the oxygen and moisture level was maintained below 0.1 ppm. All the electrochemical characterizations were performed after a quasi-equilibration time of about 8 hrs. The cyclic voltammograms and impedance analysis (EIS) was recorded using the Autolab (GPES & FRA, PGSTAT 302N) work station, and the reversible lithium insertion/extraction based life cycle study was studied by employing the WonAtech (WBCS3000S) battery tester under galvanostatic mode.

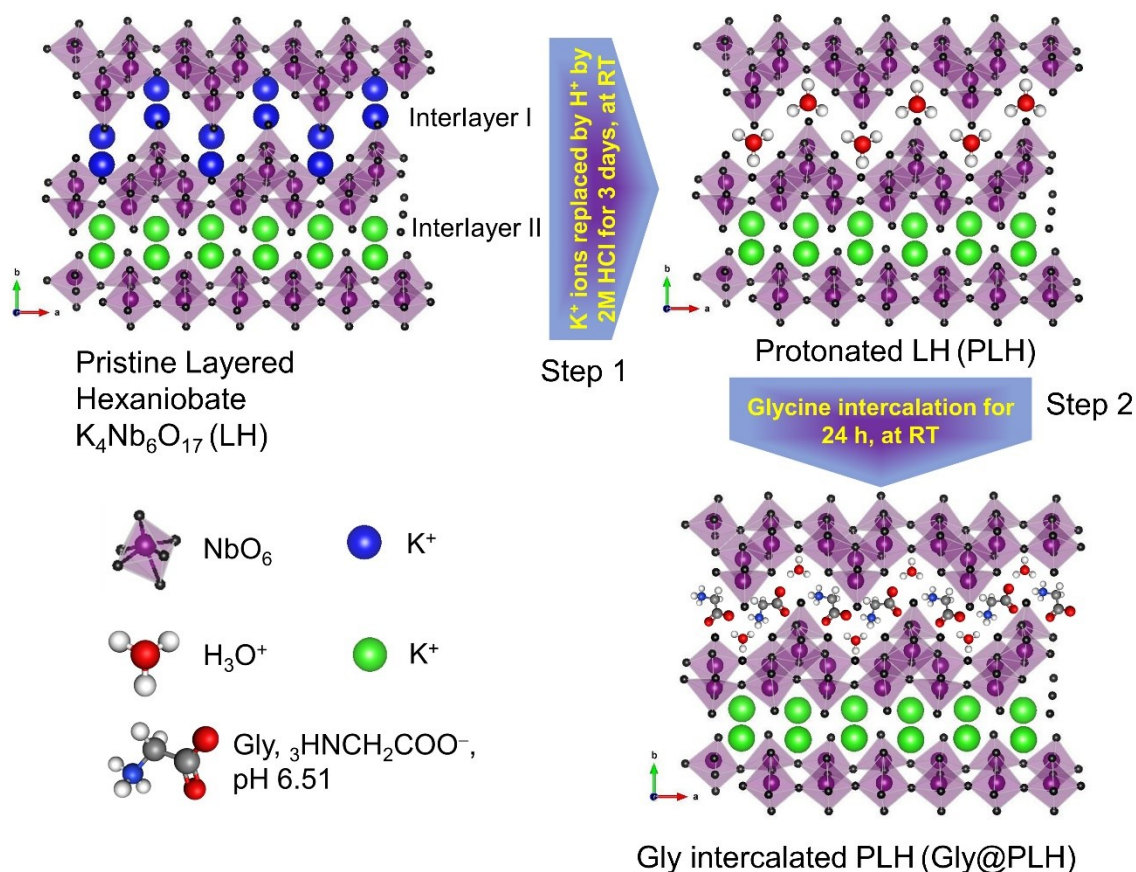


Figure. S1. The schematic representation of protonation (step 1) and subsequent Gly intercalation (step 2) of layered hexaniobate of $K_4Nb_6O_{17}$ (LH). The LH is composed of stacked negatively charged layered sheets (slabs), and the cations (K^+) occupying in both interlayer space of slabs, which are designated as interlayer-I (hydrophilic) and -II (hydrophobic), respectively as shown above. Since the interlayers-I is used to show crystallographically different intercalation properties that allow an exchange of cations, which depends upon the charge of the cation (such as H^+ , as H_3O^+).

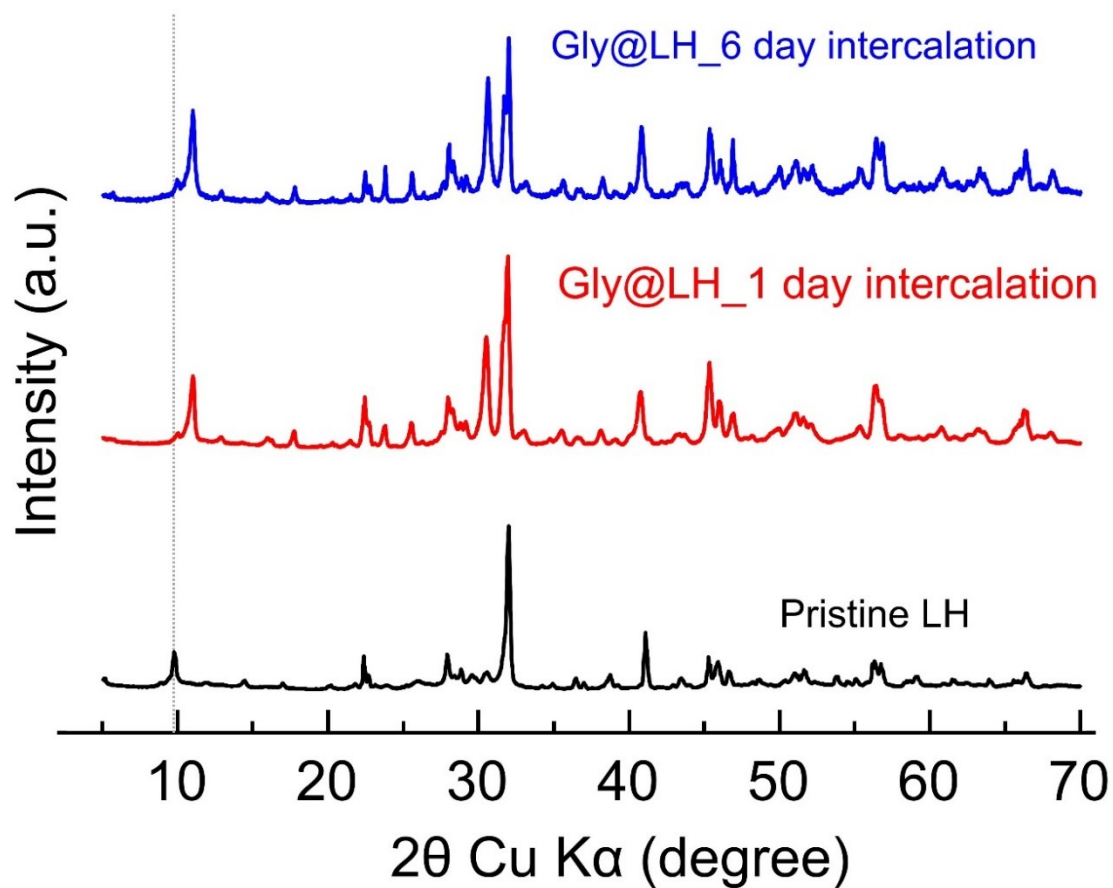


Figure S2. The powder XRD pattern of pristine LH and Gly intercalated pristine LH without protonation step for 1 day and 6 days reaction time (red and blue spectrum, respectively).

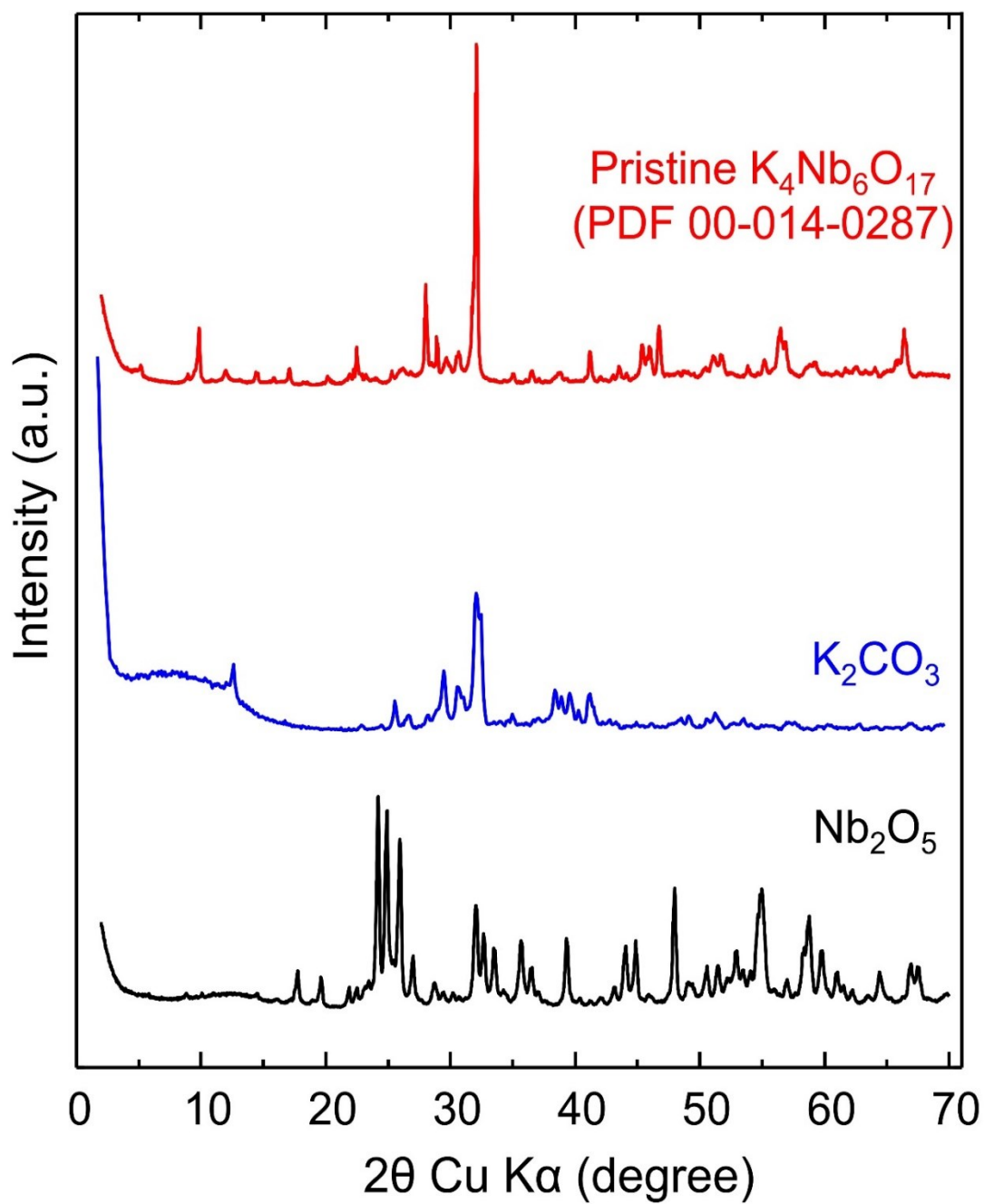


Figure S3. The powder XRD pattern of of Nb_2O_5 , K_2CO_3 and as-synthesized pristine layered hexaniobate of $K_4Nb_6O_{17}$ (LB).

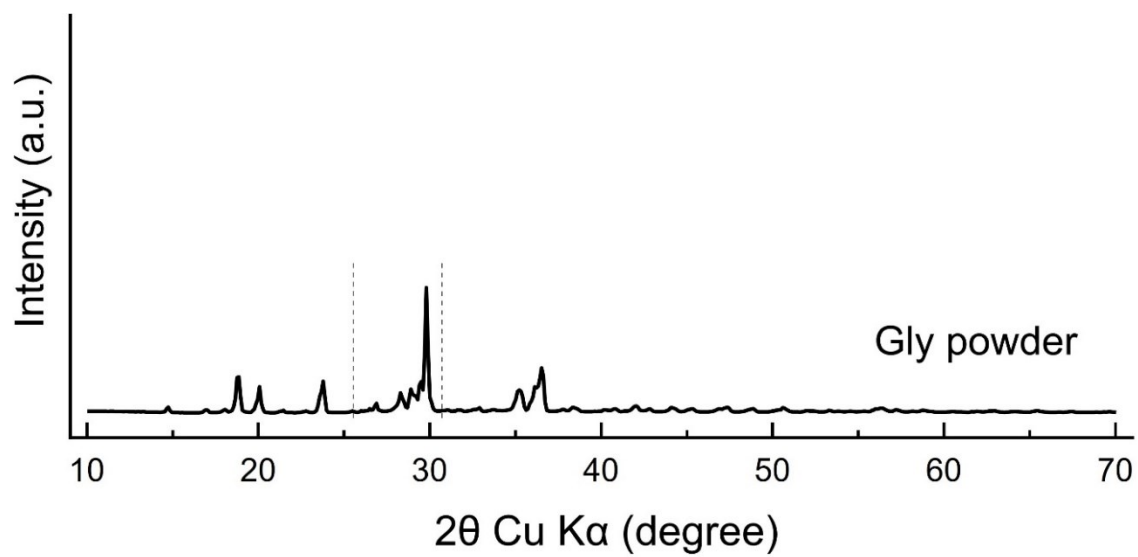


Figure S4. The powder XRD pattern of glycine powder.

IR and Raman analysis before and after intercalation of Gly (Fig. S5 and S6).

The bands at 1643, and 1547 cm^{-1} are attributed to the bending NH_2 ($\delta\text{-NH}_2$), the combinational vibrational mode of C–N symmetric stretching ($\nu_s\text{C-N}$) + N–H bending in out of phase ($\delta\text{N-H}_{\text{out of phase}}$), both are ascribed to the N–H vibrations of the amino group. The combined IR mode of $\nu\text{CO} + \delta\text{COH}$ and C–C stretching ($\nu\text{C-C}$) at 1234 and 1055 cm^{-1} , respectively. Note that the band at 2853 cm^{-1} is assigned to the $\text{N}_1\text{-H}_6$ stretching ($\nu\text{N}_1\text{-H}_6$) vibrational mode of zwitterionic species of Gly. Moreover, a strong symmetric $\nu_{\text{sym}}\text{CH}_2$, and asymmetric stretching vibrations of $\nu_{\text{asym}}\text{CH}_2$ functional group have also been detected at 2924 cm^{-1} and 2996 cm^{-1} , respectively. The vibrational bands in Fig. S5 and the Raman spectra (Fig. S6) were shown a clear distortion in niobate (NbO_6) octahedron after the proton exchange as well as Gly inclusion. In IR signature bands, the wavenumber between at 912 – 843 cm^{-1} are ascribed to the stretching of short Nb=O bonds ($\nu\text{Nb=O}$); and the band at 776 – 612 cm^{-1} attribute for the stretching of NbO_6 (νNbO_6) vibration. The combined ($\nu\text{NbO}_6 + \delta\text{NbO}_6$) mode and NbO_6 librational modes appeared between 400 – 600 cm^{-1} in both IR (Fig. S5) and Raman spectrum (Fig. S6). The vibrational spectroscopic results further confirm that the successful exchange of H^+ (as H_3O^+), and the subsequent inclusion of Gly in the interlayer-I of PLH sample since the interlayer II is chemically inactive for the functionalization (or) hybridization.

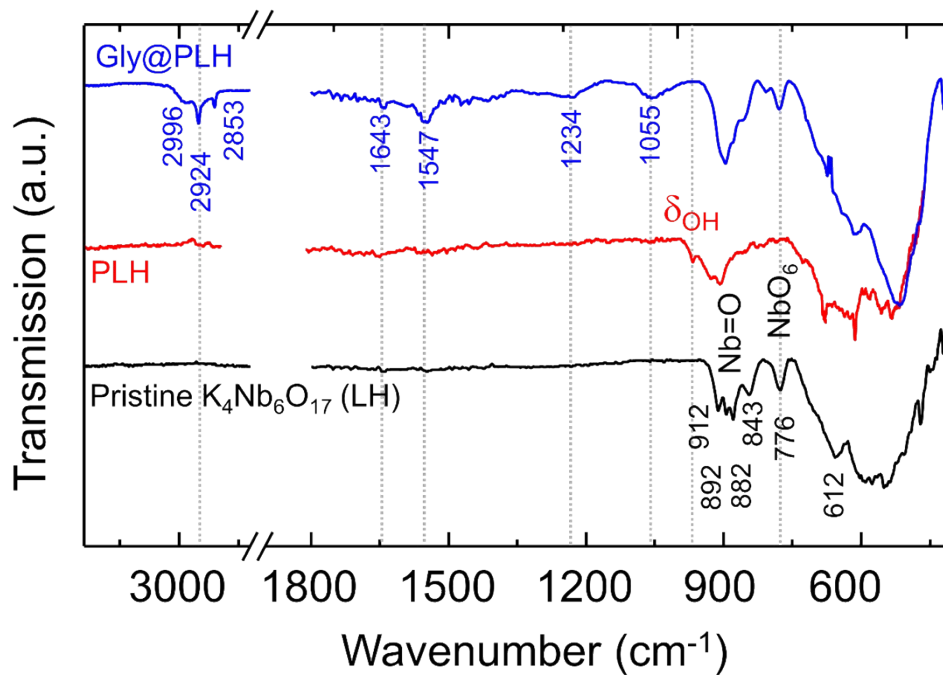


Figure S5. The Fourier transform infrared (FTIR) spectroscopy analysis of pristine LH, PLH and Gly@PLH in ATR mode.

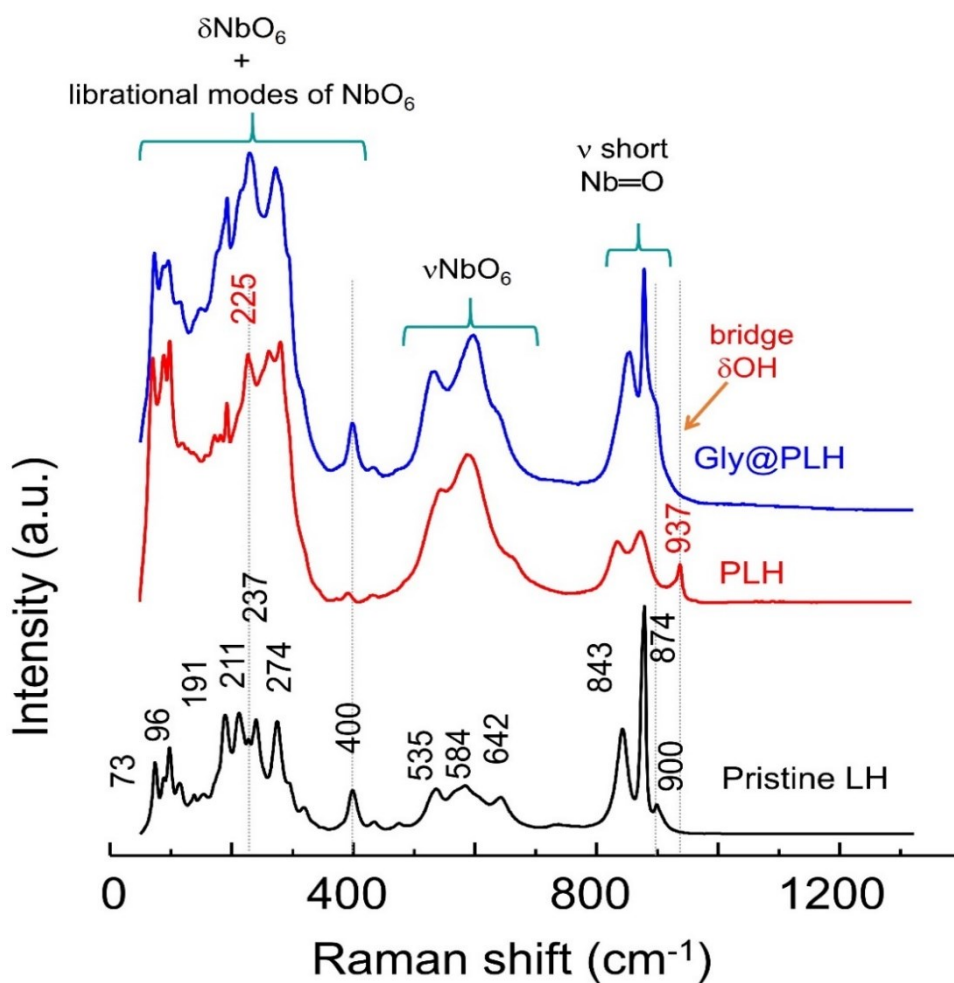


Figure S6. The Raman signature of pristine LH, PLH and Gly@PLH using 532 nm wavelength excitation laser.

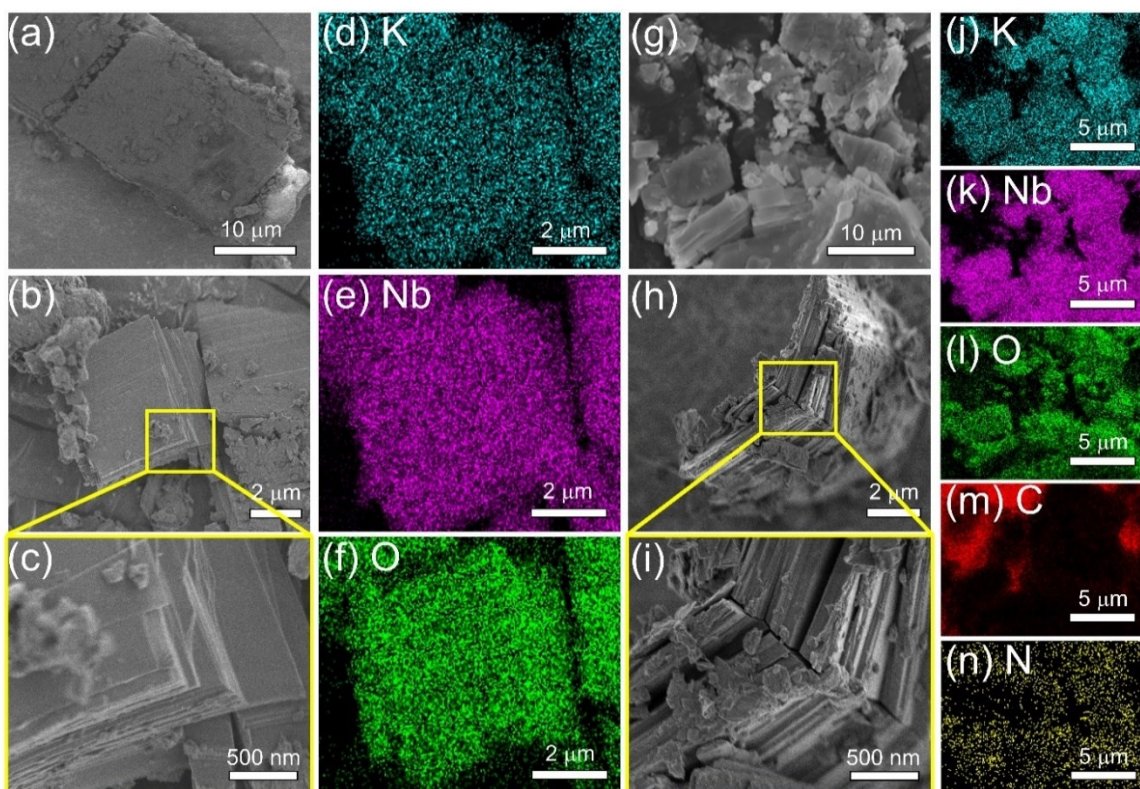


Figure S7. The FE-SEM images of LH (a-c) and Gly@PLH (g-i). The SEM images of Gly@PLH revealed that the expansion of layered structures with reduced lateral size of the niobate nanosheets is seen, whereas the pristine LH sample has exhibited a closely-stacked layered niobate nanostructure with lateral size was about 20-30 μm (Fig. 3, a-c). (j to n) The energy-dispersive X-ray (EDX) mapping images on pristine LH and Gly@PLH showed that the homogeneous distribution of the elements of K, Nb, O, C and N present in the Gly@PLH, respectively. The mapping analysis is further evidence that Gly molecules were firmly intercalated into the protonated layered niobates structures (PLH).

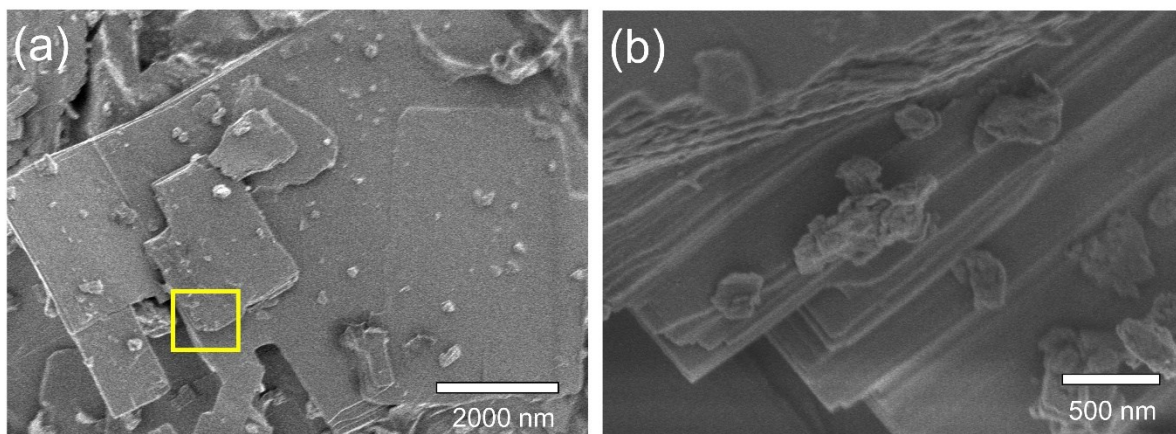


Figure S8. The low (a) and (b) resolution of FE-SEM images of Gly intercalated pristine LH without protonation step.

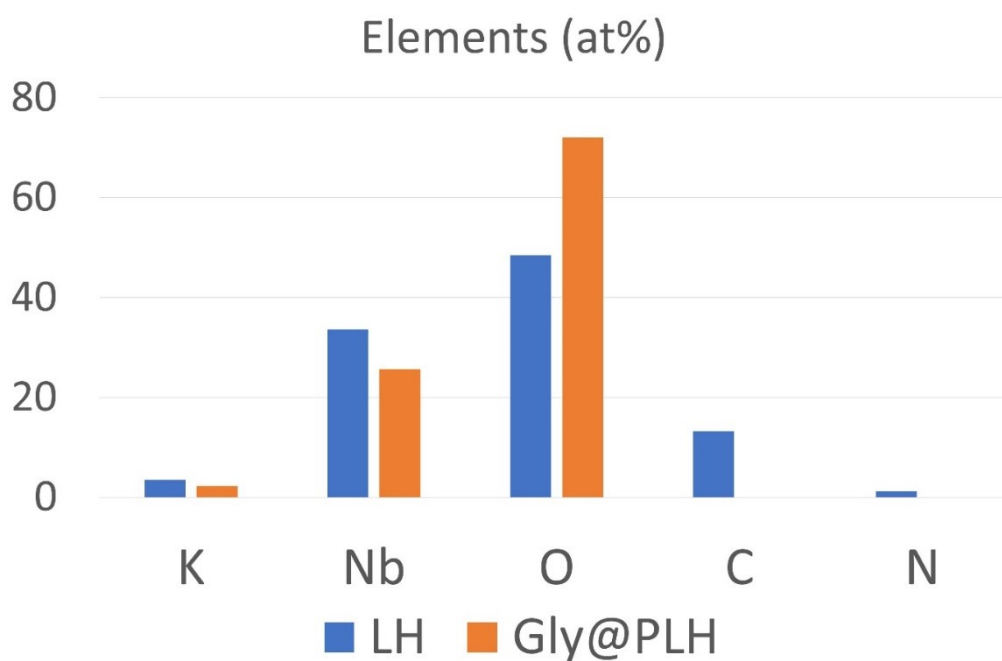


Figure S9. The percentage atomic compositions of LH and Gly@PLH sample were analyzed by STEM-EDS and Gly@PLH sample is shows the percentage atomic compositions of 3.47, 33.63, 48.46, 13.20 and 1.25 at % of K, Nb, O, C and N elements, respectively.

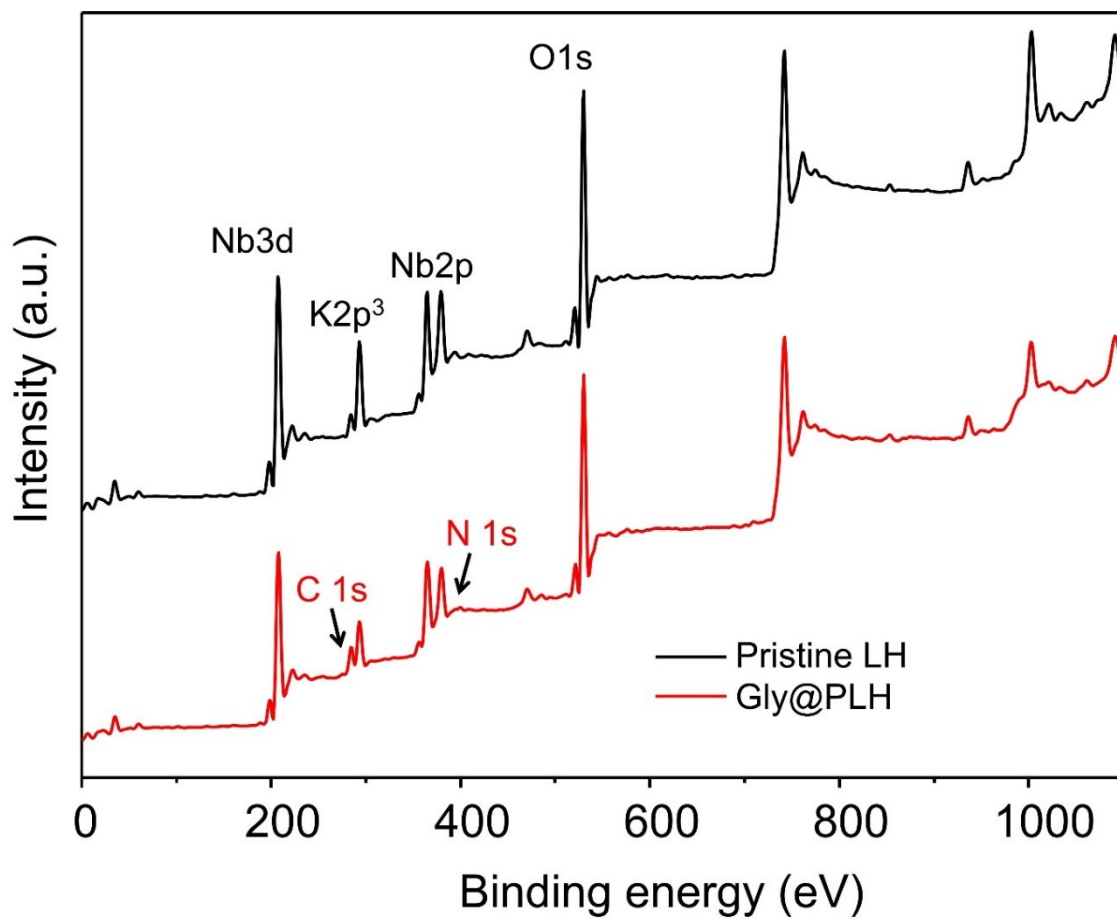


Figure S10. XPS survey spectrum of LH and Gly@PLH.

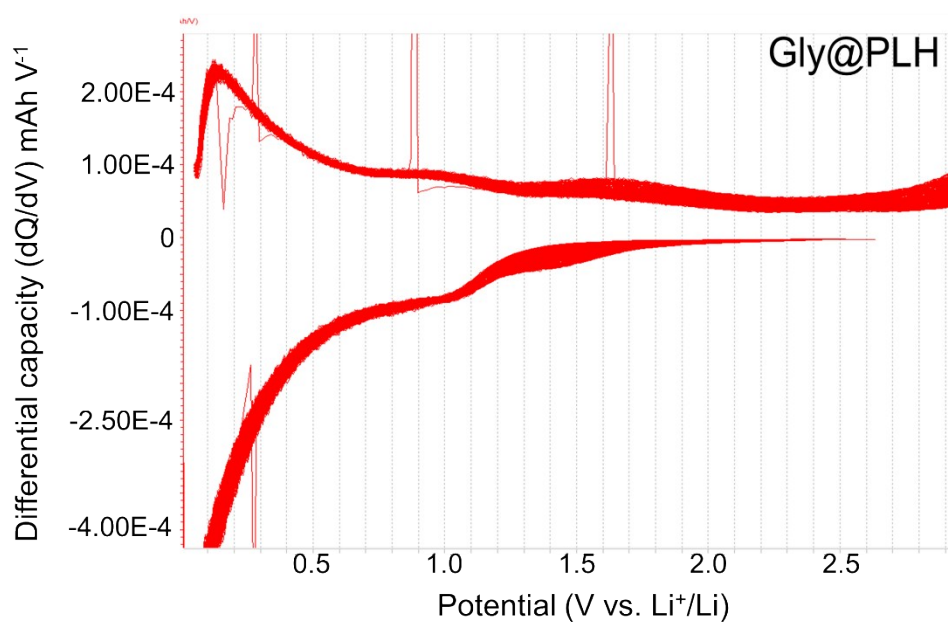
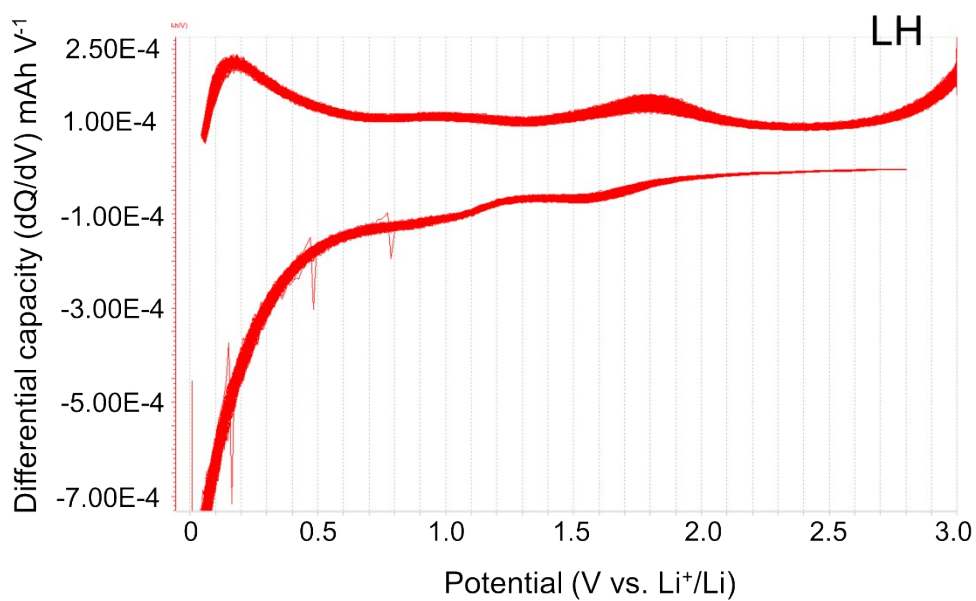


Figure S11. Comparison of selected cycles of differential capacity plot LH (left) and Gly@PLH (right) at a specific current of 0.5 A g⁻¹.

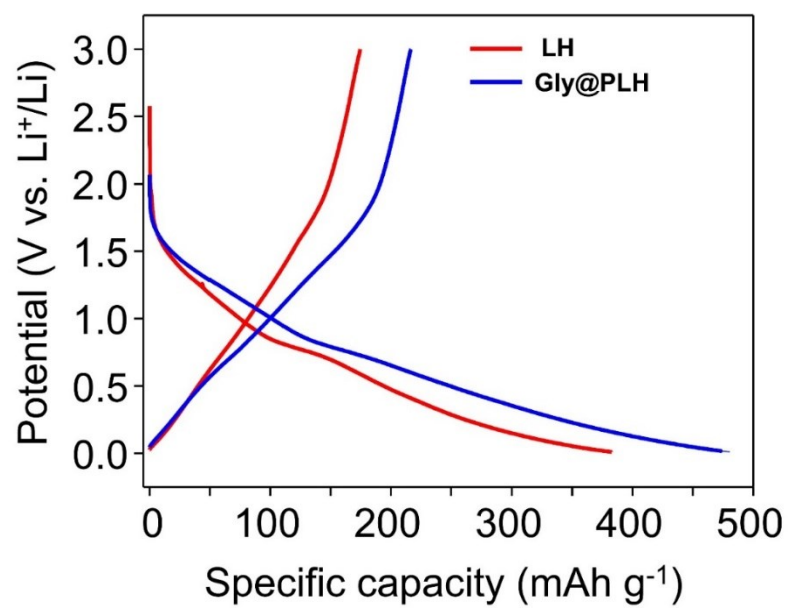


Figure S12. Normalized initial lithation plot of of LH and Gly@PLH at a specific current of 0.05 A g⁻¹.

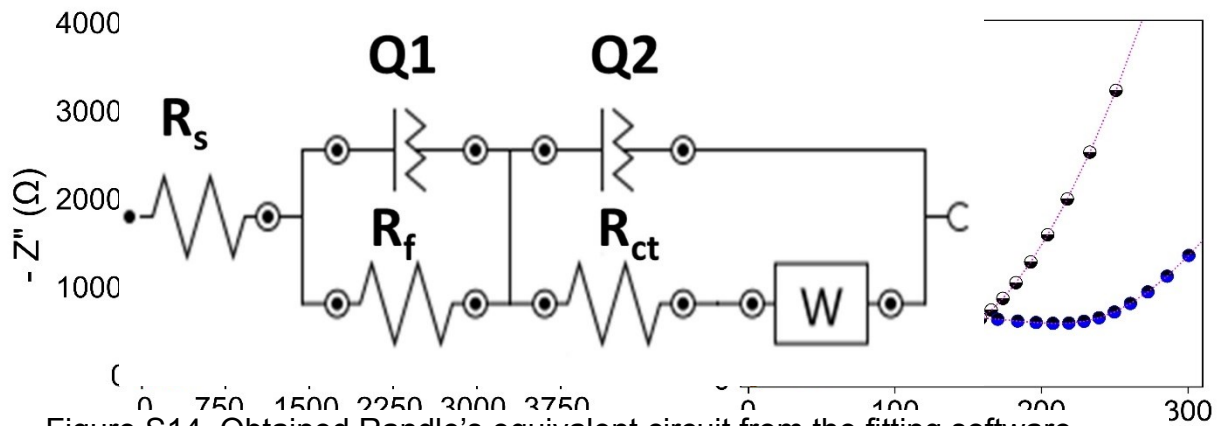


Figure S14. Obtained Randle's equivalent circuit from the fitting software.

Figure S13. Comparison of Nyquist plots before and after life-cycle study along with fitting.

